

hence, apomorphic for Neognathae.

Definitive fossils of dinosaur eggs and nests were discovered in the early 1920s. The most common type of eggs were initially identified as belonging to the ornithischian dinosaur *Protoceratops* (21). This referral was based on the abundance of both *Protoceratops* skeletal remains and this type of egg at Bayn Dzak. No undoubted embryonic remains were found in these eggs. Although embryonic remains were initially reported (22), these observations have been shown to be erroneous (23).

On the basis of circumstantial evidence, two recent studies of dinosaur eggs (1, 2) suggested that this type of egg is not from *Protoceratops*, but from a theropod dinosaur. The type of egg most common at the Flaming Cliffs is identical in size and shape, surface ornamentation, and microstructure to the egg containing the oviraptorid embryo. Hence, we now provisionally identify these as oviraptorid theropods. However, considering that embryos within eggs are scarce, the possibility that this type of egg has a broad distribution among Dinosauria cannot be discounted, although this possibility is unlikely.

Further evidence for the identification of the Flaming Cliffs eggs comes from remarkable and suggestive associations (16, 24). In 1923, George Olson collected a dinosaur nest (AMNH 6508) of this type of egg (Fig. 3) at the Flaming Cliffs. During excavation, the holotype of *Oviraptor philoceratops* (AMNH 6517) was discovered lying on top of the clutch of eggs, separated by only 10 cm. In his description of this species, Osborn surmised that this animal died while feeding on the eggs—hence the generic name he gave it, meaning “egg seizer” (16). Our evidence suggests that the holotype of *Oviraptor philoceratops* perished not while feeding on these eggs, but perhaps while incubating or protecting this clutch of eggs. Since this discovery, another such association of an adult oviraptorid and a nest of this type of egg has been reported from Djadokhta-like beds at Bayan Mandahu (24).

The abundance of this type of egg at the Flaming Cliffs, comprising approximately 50% of the eggs (1, 2) encountered, is surprising because skeletal remains of oviraptorids and other theropods are extremely rare. The original collections from the Flaming Cliffs by the Central Asiatic expeditions include 101 specimens of *Protoceratops andrewsi* (22), but only one specimen of *Oviraptor philoceratops*, two specimens of *Velociraptor mongoliensis*, and one of *Sauromithoides mongoliensis* (16). This is a strong warning against the identification of eggs only on the basis of the relative abundance of eggs and skeletons in the same horizon.

The occurrence of the tiny skulls of dromaeosaurids in association with the ovi-

raptorid egg is an enigma. Skulls of non-avian theropods this small are rare, and the close association of two specimens with the egg of another taxon is unlikely to be due to chance alone. Although they are certainly from animals close to hatchling age, it is unclear whether they are embryos or neonates; the possibility that the dromaeosaurids are from an adjacent nest, were prey items of adult oviraptorids, were predators on the oviraptorid eggs or hatchlings, or even that one of the two taxa was a nest parasite, cannot be discounted. In any case, their intimate association with the oviraptorid eggs provides another reason for caution in identifying eggs on the basis of their associations with embryos not actually enclosed within them.

REFERENCES AND NOTES

1. K. Sabbath, *Acta Palaeontol. Pol.* **36**, 151 (1991). We use the word “embryo” in cases where the fossils are sufficiently preserved to discern that the eggs had been fertilized, but the word “egg” where evidence of development is absent or equivocal.
2. K. E. Mikhailov, *ibid.*, p. 193.
3. A. Elzanowski, *Palaeontol. Pol.* **42**, 147 (1981).
4. A. V. Sochava, *Paleontol. J.* **6**, 527 (1972).
5. M. Novacek, *J. Vertebr. Paleontol.*, in press.
6. R. Gradzinski, Z. Kielan-Jaworowska, T. Maryanska, *Acta Geol. Pol.* **27**, 281 (1977).
7. T. Jerzykiewicz and D. A. Russell, *Cretaceous Res.* **12**, 345 (1991).
8. J. Lillegraven and M. C. McKenna, *Am. Mus. Novit.* **2840**, 68 (1986).
9. R. Barsbold, T. Maryanska, H. Osmolska, in *The Dinosauria*, D. Weishampel, P. Dodson, H. Osmolska, Eds. (Univ. of California Press, Berkeley, 1990), pp. 249–258.
10. H. R. Schinz and R. Zangerl, *Denkschr. Schweiz. Naturforsch. Ges.* **72**, 117 (1937).
11. M. Jollie, *J. Morphol.* **100**, 389 (1957); G. H. Schumacher and E. Wolf, *Morph. Jahrb.* **110**, 520 (1967).
12. The absence of a prefrontal bone in these specimens contradicts the idea (15) that the prefrontal bone is fused to the lacrimal and frontal bones in dromaeosaurids. Instead, we view the absence of a prefrontal bone in many theropods and birds as a derived character.
13. J. A. Gauthier, *Calif. Acad. Sci. Mem.* **8**, 1 (1986).
14. H. Osmolska and R. Barsbold, in *The Dinosauria*, D. Weishampel, P. Dodson, H. Osmolska, Eds. (Univ. of California Press, Berkeley, 1990), pp. 259–268.
15. P. J. Currie, *J. Vertebr. Paleontol.*, in press.
16. H. F. Osborn, *Am. Mus. Novit.* **144**, 1 (1924).
17. H.-D. Sues, *Can. J. Earth Sci.* **14**, 587 (1977); P. J. Currie, *J. Vertebr. Paleontol.* **7**, 72 (1987).
18. S. M. Kurzanov and K. E. Mikhailov, in *Dinosaur Tracks and Traces*, D. D. Gillette and M. G. Lockley, Eds. (Cambridge Univ. Press, Cambridge, 1989), pp. 109–113.
19. K. F. Hirsch and B. Quinn, *J. Vertebr. Paleontol.* **10**, 491 (1990).
20. K. E. Mikhailov, in *Papers in Avian Paleontology Honoring Pierce Brodkorb*, K. E. Campbell, Ed. (Natural History Museum of Los Angeles County Science Series 36, Los Angeles, 1992), pp. 361–373.
21. V. van Straelen, *Am. Mus. Novit.* **173**, 1 (1925).
22. B. Brown and E. M. Schlaikjer, *Ann. N.Y. Acad. Sci.* **40**, 133 (1940).
23. Z. Dong and P. Currie, *Can. J. Earth Sci.* **30**, 2248 (1993).
24. P. J. Currie, S. J. Godfrey, L. Nessov, *ibid.*, p. 2255.
25. G. Paul, *Predatory Dinosaurs of the World* (Simon and Schuster, New York, 1988).
26. Supported by NSF grants DEB 930070 and DEB 9407999, IREX, the Philip M. McKenna Foundation Inc., and the Frick Laboratory Endowment. We thank E. Lamm, J. Horner, P. Currie, M. Ellison, S. Park, P. McKenna, J. Lanns, B. Barnett, O. Rieppel, T. Boldskuh, and D. Baatar. This is contribution 9 of the Mongolian–American Museum of Natural History paleontological project.

22 June 1994; accepted 25 August 1994

Autumn Bloom of Antarctic Pack-Ice Algae

C. H. Fritsen,* V. I. Lytle, S. F. Ackley, C. W. Sullivan†

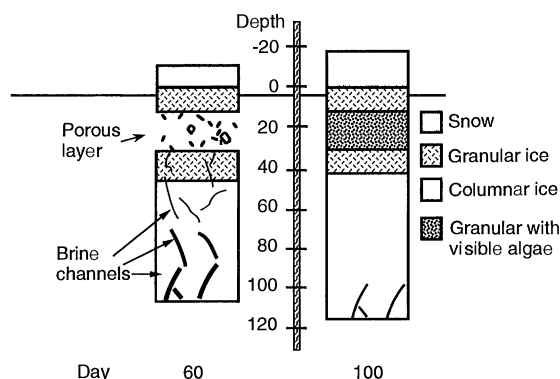
An autumn bloom of sea-ice algae was observed from February to June of 1992 within the upper 0.4 meter of multiyear ice in the Western Weddell Sea, Antarctica. The bloom was reliant on the freezing of porous areas within the ice that initiated a vertical exchange of nutrient-depleted brine with nutrient-rich seawater. This replenishment of nutrients to the algal community allowed the net production of 1760 milligrams of carbon and 200 milligrams of nitrogen per square meter of ice. The location of this autumn bloom is unlike that of spring blooms previously observed in both polar regions.

Approximately 3 to 4 × 10⁶ km² of the western sector of the Antarctic Weddell Sea is continuously covered by sea ice (1). Low water column biomass and light limitations imposed by the ice and snow restrict primary production in the water column, and dense microbial communities associated with the sea ice are presumed to be the major source of primary production for this region's pelagic ecosystem (2). Elucidating the annual production cycle and the factors controlling primary production in this region of the world ocean has been problematic because of the difficulties associated

with conducting long-term investigations in drifting pack ice. The deployment in 1992 of the first Antarctic drifting ice station (ISW-1) enabled us, however, to examine in situ microalgal production and nutrient dynamics in relation to changing physicochemical conditions in Antarctic pack ice over a prolonged period.

ISW-1 was deployed on a 2- to 3-km² multiyear ice floe (ice surviving a summer melt season) in the southwest Weddell Gyre in a region of 80 to 90% multiyear ice coverage (3). Several experimental quadrats were monitored (4) as the station drifted

Fig. 1. Stratigraphic representation of ice cores obtained from site B. Ice cores obtained throughout the multiyear ice floe often contained differing crystallographic structures; however, surface flooding and porous layers were common, and large brine drainage features were always present below the freezing front (Fig. 2). Depths (in centimeters) are relative to the ice-snow interface.



northward at 53°W longitude from 71.4°S (9 February) to 65.8°S (6 June). Results are presented from a primary 20 by 20 m study quadrat (site B) located 40 to 50 m from the perimeter of the floe in a larger area (about 0.2 km²) of relatively undeformed (0.95 to 1.2 m thick) multiyear ice. Initially, there was a layer of highly porous, unconsolidated ice (brine volume, 50 to 80%) (5) located ~5 to 10 cm below the ice-snow interface just below sea level (Fig. 1). These porous layers near sea level have been described (6) and are believed to originate by either internal melting (7) or surface flooding and infiltration of seawater into the snow, followed by freezing (6). Granular ice crystals were located above and immediately below the porous layer, and the bottom 60 to 70 cm were composed of vertical columnar crystals. Large brine channels (0.5 to 3.0 cm in diameter) permeated both the granular ice and the columnar ice below the unconsolidated layer.

Ice temperatures were initially isothermal, ranging from -1.70° to -1.80°C, and brine salinities were 30 to 34 parts per thousand (ppt). As air temperatures decreased, a freezing front propagated into the snow and sea ice (Fig. 2). The freezing front took about 2 weeks to advance 30 cm and pass through the porous layer, and an additional 2 weeks to advance the remaining 80 to 90 cm to the bottom of the ice. Coincident with the propagation of the freezing front, the ice was desalinating. By day 74 (14 March), bulk salinities of the porous layer showed that considerable desalination had occurred (Fig. 3A) despite the presence

of 80 cm of consolidated ice beneath the porous layer. The porous layer solidified as granular crystals distinguishable as a discrete band of golden-brown color caused by the presence of a dense microalgal community (Fig. 1).

Plant pigments (chlorophyll a and phaeopigments) in the ice initially ranged from 0.7 to 11 mg m⁻³, whereas water column biomass remained below 0.1 mg m⁻³ throughout the study. Standing stocks of pigments in the ice were increasing at a rate of 0.8 mg m⁻² day⁻¹ during the initial 3 weeks (day 60 to 81; Fig. 3B). Within the porous layer, carbon was fixed at rates of 100 mg of C m⁻³ day⁻¹ (day 60) and ranged up to 800 mg of C m⁻³ day⁻¹ (day 67). Integration of these rates over the 22 cm of the porous layer yields 22 to 176 mg of C m⁻² day⁻¹. The net algal C and N accumulations were equivalent to 57 mg of C m⁻² day⁻¹ and 6.3 mg of N m⁻² day⁻¹ (8). After day 81, both the in situ incubations and the changes in integrated pigments showed that the algal communities continued to grow, albeit at one-tenth of the rates before day 81. The decreases in algal growth rates were coincident and likely caused by the decreasing ice temperatures (Fig. 2), the concomitant increasing brine salinities (9), and the decreasing daily insolation.

The net production of algal biomass within the multiyear sea ice during the period of study was equivalent to 1760 mg of C m⁻² and 200 mg of N m⁻². The primary area of algal growth was in the upper 0.4 m of the ice, near the region of the porous layer, as is demonstrated by the final vertical profile of plant pigments obtained on the last day of study at this site (Fig. 3C). The increase in algal biomass at the depth of the maximum amount of pigment accumulation represented an increase of 73 mmol m⁻³ of algal nitrogen biomass. The brine initially contained only 1.9 mmol of N m⁻³ as nitrate + nitrite and 1.5 to 2.4 mmol of N m⁻³ as ammonium ion. For ice with a 50 to 80% brine content, the combined nitrogen sources would have support-

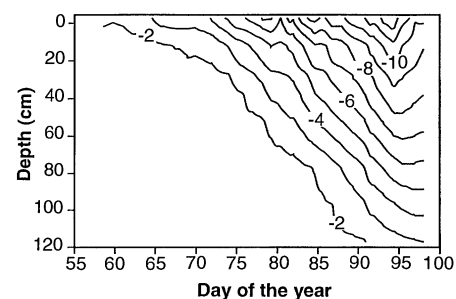


Fig. 2. Propagation of a freezing front into multiyear sea ice. Temperatures to the left of the -2°C isotherm fluctuated between -1.70° and -1.87°C. Ice thickness was 1.2 m (Fig. 1).

ed less than 5% of the observed increase in algal biomass. This nutrient deficit suggests that brine and nutrient-rich seawater exchanged during the study.

Convective brine motion has been demonstrated in laboratory-grown ice and in the bottom skeletal layers of growing landfast ice (10). In the present study, however, the density instability in the brine was formed by the rejection of brine from the new ice forming within the porous layer. Ice temperatures (Fig. 2) indicate that the brine below the freezing front never exceeded 35 to 36 ppt (9), which shows that the salts expelled from the freezing front were diluted to salinities 1 to 2 ppt greater than that of the underlying seawater. While the freezing front was advancing and the algal community was growing, concentrations (relative to salinity) of nitrate + nitrite increased within the brine and ice (Fig. 3D). By day 81, ratios of nitrate + nitrite to salinity had increased to values similar to those in the water column. This relative nutrient increase shows that the interstitial brine was mixing with nutrient-rich seawater at a rate exceeding the rate at which the algal communities used the new nutrients. After the aqueous portion of the porous layer froze and brine volumes dropped below 5%, ratios of nitrate + nitrite to salinity decreased as would be expected if the brine pockets became isolated (11) and the algal communities continued to use and deplete the trapped nutrients.

During the initial 21 days of algal growth, fluxes of seawater had to exceed 0.015 m³ m⁻² day⁻¹ in order to sustain the growth of the algal population as well as the increase in the nutrients relative to salinity. Volume fluxes estimated from a salt-balance approach (12) exceed the nutrient demand of the algae and range from 0.04 to 0.1 m³ m⁻² day⁻¹. These estimates of brine exchange lead to the conclusion that the original brine in the porous layer (0.1 to 0.17 m³) was replaced several times (up to 20) during the autumnal freezing period. The large brine channels seen in ice

C. H. Fritsen, Department of Biological Sciences, University of Southern California, Los Angeles, CA 90089-0371, USA.

V. I. Lytle, Antarctic Cooperative Research Center, University of Tasmania, Hobart, Tasmania 7001, Australia.

S. F. Ackley, U.S. Army Cold Regions Research and Engineering Laboratory, Hanover, NH 03755-1290, USA.

C. W. Sullivan, Hancock Institute for Marine Studies, University of Southern California, Los Angeles, CA 90089-0374, USA.

*To whom correspondence should be addressed.

†Present address: National Science Foundation, Office of Polar Programs, Arlington, VA 22230, USA.

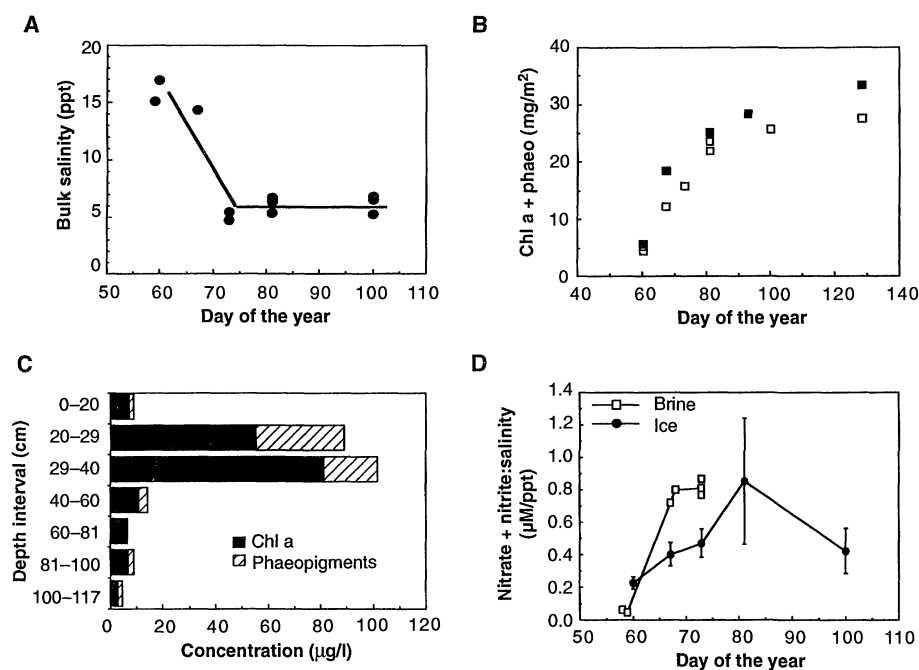


Fig. 3. (A) Bulk salinities of the porous layer [calculated as the product of the fractional brine volume (V_b) (5) and the salinity of the brine]. Points before day 74 were calculated with $V_b = 0.5$ to obtain the conservative estimate of desalination. (B) Increase in vertically integrated standing stocks of pigments [chlorophyll a (Chl a) + phaeopigments (phaeo)]. Closed symbols represent ice cores melted in filtered seawater to reduce the osmotic shock and cell lysis. Open symbols represent cores melted for nutrient analysis without the addition of filtered seawater. (C) Vertical profile of pigments on day 128. (D) Ratios of nitrate + nitrite to salinity in porous-layer brine (open symbols) and sea ice (closed symbols). Brine samples are single-sample determinations; ice values are means from five to eight sections of ice cores. Error bars, ± 2 SEM. Seawater nitrate + nitrite to salinity ratio was 0.876 ± 0.069 ($n = 8$).

cores (Fig. 1) and divers' observations of brine channels in the region lead us to conclude that the vertical exchange occurred through these conduits.

Our results document a phenomenon that is widespread and may occur throughout the freezing seasons. Antarctic pack ice frequently floods with seawater from snow accumulation or deformation events or both (13). When flooded areas freeze, the process of brine exchange is initiated, and surface and internal algal communities are presented with additional nutrients for sustained growth. In our study, sufficient light was available as the freezing front propagated into the ice for an algal bloom to occur. Dense internal bands of algae (20 to 130 mg of chlorophyll a per cubic meter) were found throughout the ISW-1 floe and in ice surveyed from ships throughout the region, which suggests that internal blooms are common.

Our results also raise some fundamental questions regarding annual production cycles and the physical factors controlling production in pelagic sea-ice ecosystems. One implication of our study is that snow cover may actually augment primary production because of its propensity to create surface flooding. In contrast, in land-fast sea-ice ecosystems, snow cover has been shown only

to reduce primary production (14, 15). Spring blooms of bottom-ice algae have been considered to be the primary source of new production in the sea-ice ecosystems studied thus far (14, 15). However, in pelagic regions of perennial pack ice with deep snow cover, spring blooms of bottom-ice communities may be substantially limited by the amount of light available, and losses due to bottom ablation may be strong. Autumnal blooms, of interior and surface communities, are therefore more likely to be the primary sources of new production.

REFERENCES AND NOTES

- H. J. Zwally *et al.*, *Antarctic Sea Ice, 1973-1976: Satellite Passive-Microwave Observations* (SP-459, NASA, Washington, DC, 1983).
- J. Marra and D. C. Boardman, *Mar. Ecol. Prog. Ser.* **19**, 197 (1984); S. T. Kottmeier and C. W. Sullivan, *ibid.* **36**, 287 (1987); L. Legendre *et al.*, *Polar Biol.* **12**, 429 (1992).
- A. L. Gordon *et al.*, *Eos* **74**, 121 (1993).
- Six thermistor strings were embedded in the ice and temperature profiles (from the air into the water column) were recorded hourly. Ice cores, seawater, and brine samples were collected repeatedly, and a suite of measurements was conducted that included salinity, ice texture and density (76), nitrate + nitrite (77), ammonium (78), chlorophyll a and phaeopigments (78), and particulate organic carbon and nitrogen (79). In situ ^{14}C -bicarbonate incubations also were conducted within the multiyear ice to determine rates of primary production and algal growth in situ (75).
- Fractional brine volumes, V_b , of the unconsolidated

porous layer (Fig. 1) were estimated as $V_b = 1 - V_{mw} V_{ps}^{-1} \epsilon^{-1}$, where V_{mw} is the volume of the melt water from unconsolidated ice crystals collected from a known volume of porous-layer ice, V_{ps} and ϵ is the volume expansion coefficient of ice. When the ice was consolidated, V_b was calculated according to the method of G. F. N. Cox and W. F. Weeks [*J. Glaciol.* **32**, 371 (1986)].

- S. T. Kottmeier and C. W. Sullivan, *Deep Sea Res.* **37**, 1131 (1990); S. F. Ackley and C. W. Sullivan, *ibid.*, in press.
- V. K. Buynitsky, *Oceanology* **8**, 771 (1968).
- Ratios of C and N to chlorophyll a + phaeopigments (w/w) were determined by linear regression analysis (\pm SEM) [K. Banse, *Mar. Biol.* **41**, 199 (1977)] and corroborated by measurements of total algal cell volume to chlorophyll a ratios [R. R. Strathman, *Limnol. Oceanogr.* **12**, 411 (1967)]. Carbon to chlorophyll a + phaeopigment ratio = 70.7 ± 10.2 ; nitrogen to chlorophyll a + phaeopigment ratio = 7.9 ± 0.789 .
- A. Assur, in "Arctic sea ice" (Publication 598, National Research Council, Washington, DC, 1958), p. 14.
- R. A. Lake and E. L. Lewis, *J. Geophys. Res.* **75**, 583 (1970); L. I. Eide and S. Martin, *J. Glaciol.* **14**, 137 (1975); T. M. Neidrauer and S. Martin, *J. Geophys. Res.* **84**, 1176 (1979); W. S. Reeburgh, *Polar Biol.* **3**, 29 (1984); K. R. Arrigo, J. N. Kremer, C. W. Sullivan, *J. Geophys. Res.* **98**, 6929 (1993).
- Isolation of brine pockets occurs at $V_b \leq 0.05$ [H. Eicken, *J. Geophys. Res.* **97**, 15545 (1992)].
- The desalination rate of the porous layer is the difference between the loss and gain of salts in the exchange of brine (S_b) and seawater (S_{sw}), such that $V_i(S_{io} - \epsilon S_{if})t^{-1} = Q_{in} S_b - Q_{out} S_{sw}$, where S_{io} and S_{if} are the initial (17 ppt) and final (6 ppt) bulk salinities of the layer (Fig. 3A), V_i is the thickness (0.22 m) of the porous layer, t is the time (days) during which the layer froze, Q_{in} and Q_{out} are the volume fluxes ($\text{m}^3 \text{m}^{-2} \text{day}^{-1}$) into and out of the layer, and ϵ is the volume expansion coefficient of water (dimensionless). Because water expands as it freezes, the volume flux of brine out of the layer is slightly more than the flux into the layer by $Q_{out} = Q_{in} + (1 - \epsilon)Q_{ice}$, where Q_{ice} is the rate of ice growth ($\text{m}^3 \text{m}^{-2} \text{day}^{-1}$) within the porous layer. Substituting into the first equation and solving for Q_{in} we get:

$$Q_{in} = [V_i(S_{io} - \epsilon S_{if})t^{-1}] - [(1 - \epsilon)Q_{ice}S_b] / (S_b - S_{sw})^{-1}$$
- From the thermistor profiles, $S_b - S_{sw} = 1$ to 2 ppt, and for the 21 days for the freezing of the porous layer, $Q_{in} = 0.04$ to $0.1 \text{ m}^3 \text{m}^{-2} \text{day}^{-1}$.
- M. A. Lange *et al.*, *J. Glaciol.* **36**, 315 (1990); H. Eicken, M. A. Lange, H. Hubberten, P. Wadhams, *Ann. Geophysicae* **12**, 80 (1994).
- H. E. Welch and M. A. Bergmann, *Can. J. Fish. Aquat. Sci.* **46**, 1793 (1989); K. R. Arrigo, J. N. Kremer, C. W. Sullivan, *J. Geophys. Res.* **98**, 6929 (1993).
- S. M. Grossi *et al.*, *Mar. Ecol. Prog. Ser.* **35**, 153 (1987).
- A. J. Gow, S. F. Ackley, W. F. Weeks, J. W. Govoni, *Ann. Glaciol.* **3**, 113 (1982).
- C. M. Sakamoto, G. E. Friedrich, L. A. Codispoti, *Technical Report 90-2* (Monterey Bay Aquarium Research Institute, Pacific Grove, CA, 1990).
- T. R. Parsons, Y. Maita, C. M. Lalli, *A Manual of Chemical and Biological Methods for Seawater Analysis* (Pergamon, Elmsford, NY, 1984).
- A Leeman Labs model CE440 automated CHN analyzer was used (MSI analytical labs, University of California, Santa Barbara).
- We thank J. Arda, C. Mordy, I. Melnikov, B. Elder, D. Bell, P. Sullivan, R. Swayzer, and all ISW-1 organizers and participants for contributing to the implementation and completion of the field work and J. Kremer, M. Gosselin, I. Allison, A. McMinn, K. Michel, J. Berwald, W. Toller, and two anonymous reviewers for comments and insightful suggestions on earlier versions of the manuscript. Supported by NSF grant DPP 90-23669 (to C.W.S.) and DPP 90-24089 (to S.F.A.).

27 May 1994; accepted 29 August 1994